Plasma Treatment to Improve the Photoelectroactivity of Sb_2S_3 Thin Films in Water Splitting

Moisés A. De Araújo[b] and Lucia H. Mascaro*[a]

The present study reports a novel and fast nitrogen plasma treatment approach to boost hydrogen evolution on antimony (III) sulfide (Sb_2S_3) thin films via light-driven water splitting. The Sb_2S_3 films were synthesized by electrodepositing antimony followed by sulfurization, and then using different treatment times under nitrogen plasma. The plasma treatment time did not result in significant changes in the microstructural and optical properties, compared to the non-plasma films. However, the wettability drastically changed from superhydrophobic for the non-plasma film to hydrophilic once treated. Photoelectrochemical analysis showed a substantial photocurrent density increase (24-fold) for the film treated for 10 s in comparison with the non-plasma film. Further characterization by X-ray photoelectron spectroscopy and scanning electron microscopy revealed chemical and morphological modifications for the films treated, which explain the enhancement of photoelectroactivity and wettability.

1. Introduction

A shortage of fossil fuel in the future, associated with the environmental impact caused by the immense use of this material, have compelled a rush to seek out new energy sources which will classify as renewable, abundant, sustainable, and environmentally benign. Potentially, the sun appears to be the energy source that complies with such requirements and can effectively overcome the world's energy issues as the average rate of solar energy reaching the earth's surface is ca. 10,000 times higher than the rate of energy consumption worldwide by humans.[1] Due to this copious amount of energy, semiconductors feature as attractive materials to harvest solar energy into chemical energy such as hydrogen energy, which is a sustainable and clean energy. A number of semiconductor materials have been under consideration for hydrogen gas (H_2) production via water splitting in photoelectrochemical cells (PECs). Among them, antimony sulfide (Sb_2S_3) stands out as an earth-abundant, low toxicity, and low-cost material with fine structural and optoelectronic properties for PEC applications.[2,3] Furthermore, Sb_2S_3 is reported as being either an n- or p-type semiconductor material depending on the experimental conditions.[4] This dual conductivity behavior probably arises from the existence of antimony (Sb) or sulfur (S) vacancies.[4] Sb_2S_3 possesses a remarkable absorption coefficient (α) of around 10^4–10^5 cm^{-1} (for photons having energy higher than its bandgap) and can harvest a significant portion of the solar spectrum as it has a narrow (allowed) direct and indirect optical bandgap (E_g) of 1.7 and 1.6 eV, respectively.[5] In addition, the conduction (−0.27 vs. RHE at pH 0[3]) and the valence (1.46 V vs. RHE at pH 0[3]) band edge potentials make this material particularly suitable to light-driven water splitting into H_2 and oxygen gas (O_2), respectively, in PECs. Despite these unique properties, bare Sb_2S_3 has only been reported as a photoanode for O_2 production[2,6] but, to the best of our knowledge, there are not yet any reports addressing bare Sb_2S_3 as a photocathode for H_2 evolution. Two studies reported a heterostructure configuration of Co_3O_4/Sb_2S_3[7] and $CuInS_2/Sb_2S_3/Pt$[8] in which Sb_2S_3 was not the main absorber layer but played the role of improving carrier separation and transportation for further photoelectrochemical performance towards H_2 evolution. Improving photoelectroactivity of Sb_2S_3 itself can be achieved by surface treatment such as a plasma treatment approach. This method has acquired great attention for its ability to introduce vacancies, conducting surface modification, or creating amorphous layers by the reaction with its ionized working gas.[9] Additionally, plasma treatment can effectively modify surface wetting behavior[10–12] which is an important aspect for efficient H_2 production in aqueous media. However, despite the importance of surface wettability for PEC applications, the very nature of this matter has not been assessed whatsoever as a result of plasma treatment of Sb_2S_3 films. Only a small number of studies based on the nitrogen plasma approach have been dedicated to analyze the optical, physical, and electrical parameters, such as the electrical resistivity and conductivity of this material.[13–15] None of the studies have evaluated the effect of nitrogen plasma treatment on the photoelectrochemical and wetting properties of Sb_2S_3 films. In the light of this, herein we propose a novel and fast methodology based on nitrogen plasma treatment of Sb_2S_3 thin films for the improvement of H_2 production via photo-assisted water splitting.

[a] Prof. Dr. L. H. Mascaro
Department of Chemistry
Universidade Federal de São Carlos
Rodovia Washington Luiz, km 235
13565-905, São Carlos – São Paulo, Brazil
E-mail: lmascaro@ufscar.br
[b] M. A. De Araújo
Department of Chemistry
Universidade Federal de São Carlos
Rodovia Washington Luiz, km 235
13565-905, São Carlos – São Paulo, Brazil

Experimental Section

The Sb_2S_3 films were obtained firstly by electrodepositing Sb films potentiostatically at −1.14 V with a deposition charge density of −500 mC cm^{-2}.[16] This experiment was carried out on a potentiostat/galvanostat (Autolab PGSTAT302N) using a three-electrode cell configuration which contained an Ag/AgCl/Cl$^-_{(sat.\ KCl)}$ (reference electrode), platinum plate (counter electrode) and a glass-coated FTO substrate (working electrode) which was previously cleaned and hydrophilized.[16] The electrodeposition bath was made up of 6.0 mmol L^{-1} $K_2Sb_2(C_4H_2O_6)_2$ (Sigma-Aldrich, ≥99%) dissolved in 0.1 mol L^{-1} $KNa(C_4H_4O_6)$ (Sigma-Aldrich, ≥99%) at pH 6.0. In a second step, the electrodeposited films were sulfurized at 300 °C for 3 h under a sulfur (Reagen) sublimed atmosphere. Finally, the Sb_2S_3 films were treated under nitrogen plasma (Zhengzhou CY-P2L-B) conditions for 5, 10 and 15 s. The plasma carrier gas was nitrogen (White-Martins, 99.99%), and the radiofrequency power imposed on was 80 W. The non-plasma film, and those treated under plasma at different span times, were microstructurally characterized using an X-ray diffractometer (Shimadzu XRD-6000) with Cu Kα radiation (1.54 Å) at a scan rate of 0.20° min^{-1}. A scanning electron microscope (Zeiss Supra™ 35) was used for surface morphology investigation. The static water contact angle measurements were based on the sessile drop method, employing a contact angle goniometer (Ramé-hart model 260 F4 series) and the DROPimage Advanced software (Ramé-hart instrument co.). The chemical surface analysis was carried out on an X-ray photoelectron spectrometer (Scienta Omicron ESCA$^+$) having an exciting source of Al Kα (1486.7 eV). The C 1s peak (284.8 eV) was used for correction of charging effects. For the spectra deconvolution, a U 2 Tougaard was employed for background, with a Lorentzian line shape LA (1.53,243). All data analyses were conducted using CasaXPS software (version 2.3.19PR1.0). A UV-Vis-NIR spectrometer (Varian Cary 5) at reflectance mode was utilized for the estimation of the optical E_g. The photoelectrochemical characterization was conducted by linear sweep voltammetry, scanned from the open circuit potential to −0.4 V in the dark, and under illumination at a scan rate of 50 mV s^{-1}. The experiment was performed in a three-electrode cell with a quartz window which contained a N_2-saturated solution comprised of 0.5 mol L^{-1} Na_2SO_4 (Sigma-Aldrich, ≥99.0%) at pH 2.0. The films were frontal illuminated with a solar simulator light (Oriel® LCS-100™ containing a 100 W xenon lamp, and an AM1.5G filter) at an irradiance of 100 mW cm^{-2}.

2. Results and Discussion

The photoelectroactivity of the Sb_2S_3 films for H_2 production as a function of the plasma treatment time was assessed by linear sweep voltammetry in the dark in 0.5 mol L^{-1} Na_2SO_4 at pH 2.0, and under a solar light simulator (Figure 1).

According to Figure 1, all the films are p-type semiconductor materials due to the detection of cathodic photocurrent density signal which is ascribed to the reduction (Eq. 2) of the hydronium ions (H_3O^+) by the photogenerated electrons in the conduction band (e^-_{CB}) of the film (Eq. 1[17]).

$$h\nu \rightarrow h^+_{VB} + e^-_{CB} \quad (1)$$

$$2H_3O^+_{(aq)} + 2e^-_{CB} \rightarrow H_{2(g)} + 2H_2O_{(l)} \quad (2)$$

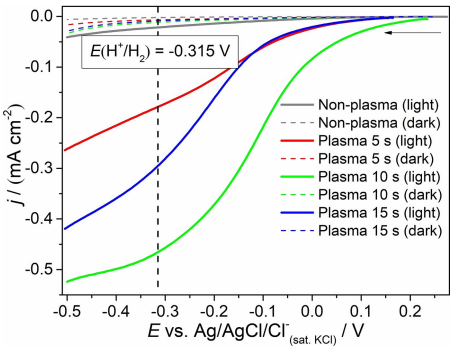

Figure 1. Linear sweep voltammograms at a scan rate of 50 mV s^{-1} in the dark, and under a solar light simulator (100 mW cm^{-2}) of the Sb_2S_3 films not subjected to plasma treatment, and those treated at different span times. The electrolyte was 0.5 mol L^{-1} Na_2SO_4 at pH 2.0.

in which *hν* is the photon energy to generate holes in the valence band (h^+_{VB}) and e^-_{CB}.

Considering the photocurrent density values at −0.315 V (dashed vertical line from Figure 1), which is the thermodynamic potential for the hydrogen evolution reaction (HER) at pH 2.0, the non-plasma film achieved a photocurrent density of −0.020 ± 0.007 mA cm^{-2}. The films treated under plasma for 5, 10 and 15 s had photocurrent density values of −0.15 ± 0.04, −0.48 ± 0.04 and −0.24 ± 0.05 mA cm^{-2}, respectively. In terms of cathode photocurrent density increments, treating under plasma for 10 s favored a 24-fold increase in photocurrent density values compared to the non-plasma treated film. However, a longer plasma treatment time of 15 s resulted in a declining photocurrent density. In order to understand the plasma treatment effect on the photoelectroactivity of Sb_2S_3 films, physical, chemical, and optical characterization has been carried out.

The microstructural nature of the non-treated Sb_2S_3 films, and those subjected to plasma treatment for different durations was revealed by means of X-ray diffraction (XRD) and the results are depicted in Figure 2a.

Based on Figure 2a, the diffraction peaks labelled with hashes (#) are ascribed to the FTO substrate, and all of the unlabeled diffraction peaks of the non-plasma film were indexed to the Sb_2S_3 phase (JCPDS n° 42–1393) which has an orthorhombic crystal system.[18] The films treated under plasma at different times had not undergone phase transformation,

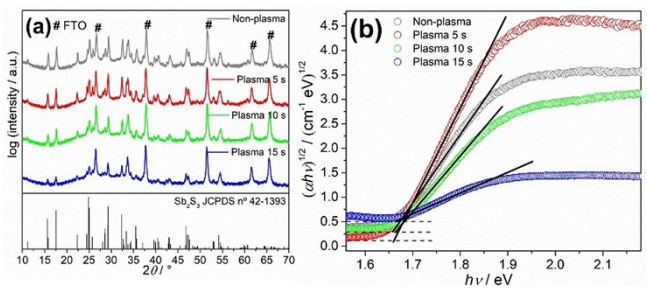

Figure 2. a) XRD patterns and b) Tauc plots of the Sb_2S_3 films not subjected to plasma treatment, and those treated at different span times.

and the Sb_2S_3 phase was also the only one detected for all samples. In addition, the crystalline nature of the films remained unaffected by the plasma treatment time as the diffraction peaks have not significantly shifted. However, the diffraction peaks of the film treated for 15 s apparently reduced intensity compared to the other plasma treating times. One of the possible reason associated with it is probably the loss of material from the film's surface by the etching effect as observed for other materials treated under plasma.[19,20] Concerning the optical characterization (Figure 2b), the estimated optical E_g of an (allowed) indirect electronic transition for the non-plasma film was 1.65 ± 0.02 eV, which is in accordance with the one reported in literature.[5] For the films treated under plasma, the E_g values (1.66 ± 0.01, 1.66 ± 0.02 and 1.67 ± 0.01 eV for the plasma treatment times of 5, 10 and 15 s, respectively) were not significantly altered compared to the non-plasma film. Such results demonstrate that the identity of the films as Sb_2S_3 remained unaltered by the plasma treatment, in accordance with the outcome observed from the XRD data (cf. Figure 2a).

Further characterization was performed with regard to the degree of wettability of Sb_2S_3 films as a function of plasma treatment time (Figure 3).

From Figure 3, the non-plasma film features as superhydrophobic as the water contact angle was $157 \pm 4°$, whilst the 5 s ($121 \pm 0.20°$) and 10 s ($47 \pm 0.14°$) plasma treated films are classified as hydrophobic and hydrophilic, respectively.[21] For the last plasma treatment time (15 s), we were not able to measure the water contact angle; however, the wettability had been improved compared to the 10 s plasma treatment time, as the contact angle seemed to be less than $47 \pm 0.14°$. Correlating these results with the photoelectroactivity assessment in Figure 1, the diminished photocurrent density value obtained for the non-plasma film is linked to the superhydrophobic nature of the film surface. It is proposed that the hydrophobic surface of chalcogenide materials in general arise from their chemical elements having alike electronegativity which gives rise to a non-polar covalently bonded network.[22] A hydrophobic surface impedes H_2 production via water splitting as it thwarts H_3O^+ ions from reaching the surface to enable the HER to take place as described by Eq. 2. The difference in photocurrent density values for the films treated for 5 and 10 s is also associated with the enhancement of the degree of wettability. An even higher photocurrent density result was expected for the film treated for 15 s as this condition allowed further surface hydrophilicity improvement, nevertheless the photocurrent density diminished (see Figure 1). This means that there is possibly another parameter beyond wettability which is playing a role in the photoelectroactivity.

To enable a broader understanding of the system, morphology analysis by scanning electron microscopy (SEM) images (Figure 4) were reviewed.

According to the SEM images in Figure 4, the non-plasma film did not resemble any particular morphology and consisted of small agglomerated particles with uneven size, in accordance with that reported in the literature.[23,24] A similar feature was observed for the films treated under plasma for 5 s. Increasing plasma treatment time to 10 s appeared to result in increasing the size of the agglomerated particles. The film treated for 15 s still presented agglomerated particles which seemed to be more dispersed from each other. In addition, a second structure featuring a sort of globular-like morphology was observed. Such dramatic morphological change for the film treated for 15 s might be the cause of the photocurrent density diminishing (see Figure 1) and possibly the wettability improvement (see Figure 3). Finally, the effect of plasma treatment time on the Sb_2S_3 films was further assessed chemically by means of X-ray photoelectron spectroscopy (XPS) (Figure 5).

As seen in Figure 5, for the film not subjected to plasma treatment, the Sb 3d high-resolution spectrum for the non-plasma film presented components at 529.3 and 529.9 eV for Sb $3d_{5/2}$, and 538.6 and 539.2 eV for Sb $3d_{3/2}$. These peaks are assigned to Sb^{3+} in Sb_2S_3.[25–27] An additional peak at 532.1 eV (O 1s) is probably attributed to adsorbed water on the film surface during air exposure.[28] The deconvoluted S 2p core level spectrum also presented four components at 161.2 and 163.4 eV for S $2p_{3/2}$, and 162.2 and 164.7 eV for S $2p_{1/2}$, which can be attributed to S^{2-} in Sb_2S_3.[26,29] The N 1s spectrum did not

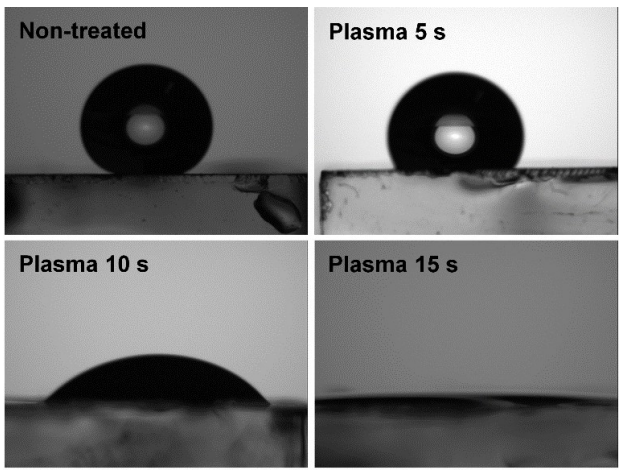

Figure 3. Water contact angle images of the Sb_2S_3 films not subjected to plasma treatment, and those treated at different span times.

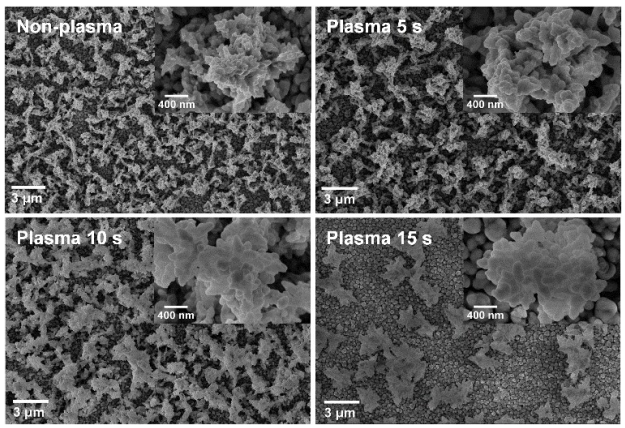

Figure 4. SEM images of the Sb_2S_3 films not subjected to plasma treatment, and those treated at different span times.

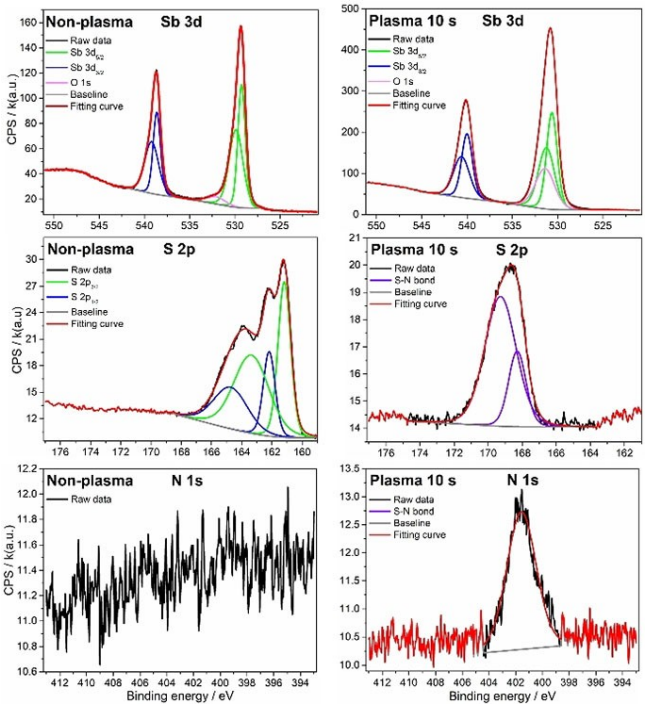

Figure 5. XPS spectra of the Sb_2S_3 films not subjected to plasma treatment, and the film treated for 10 s.

show any signal. Once the film was treated under plasma for 10 s (the condition which resulted in the highest photocurrent density), the Sb 3d spectrum did not change its profile, or the peaks' position compared to the non-plasma film. However, the O 1s peak at 531.4 eV for the treated film increased intensity. This may be linked to more adsorbed atmospheric oxygen (O_2, water vapor, etc.) in the S vacancy sites which can be formed from the ejection of S atoms by the plasma bombardment.[30] The profile of the S 2p and N 1s spectra presented substantial changes after plasma treatment. The peaks at 168.3 and 169.3 eV for S 2p, and 401.6 eV for N 1s are most likely assigned to nitrogen bonded to sulfur.[31] It is noteworthy to mention that although the N 1s spectrum reported here overlaps with the one for the antimony(III) nitride (SbN_3) which is 401.8 eV (N 1s),[32] the binding energy peaks from the Sb 3d spectrum of SbN_3 (539.6 and 530.2 eV for Sb $3d_{5/2}$ and $3d_{3/2}$, respectively[32]) differ in position compared to those presented here for the film treated under plasma for 10 s (530.8 and 540.2 eV for Sb $3d_{5/2}$ and $3d_{3/2}$, respectively). Further chemical characterization of the nitrogen plasma by Calixto-Rodriguez et al.[14] using optical emission spectroscopy demonstrated the existence of N_2^+ and NS species among others, which originated from the interaction of the nitrogen plasma with the Sb_2S_3 surface. The authors have not observed the formation of Sb-N species.[14] These reported results are additional evidence supporting our XPS data that the nitrogen ions from the plasma are very likely to be bonded to sulfur of the Sb_2S_3 film surface. Additional analysis in terms of the N/S atomic ratio also indicated an increase of N content on Sb_2S_3 surface over plasma treatment time as the films treated for 5, 10 and 15 s presented N/S values of 0.25, 0.41 and 0.56, respectively.

Having in mind all these results and that plasma is an ionized gas containing an assemblage of charged particles (electrons, ions, photons, excited and neutral species, etc.) which are highly energetic and reactive.[19] It is very likelihood that the bombardment of these reactive species such as nitrogen ions onto the Sb_2S_3 film resulted in their incorporation as S–N bonds on the film's surface. The introduction of nitrogen specie upon materials' surface by nitrogen plasma treatment was also reported for other chalcogenides[33–35] as well as polymers.[36] Albeit the mechanism behind the S–N bond formation by the nitrogen plasma interaction is still not well understood, we believe that the steps involved are the cleavage of the sulfur bonds by the nitrogen ion collisions and the subsequent S–N bond formation as similarly reported for other systems.[19,37] The presence of a polar group such as S–N[38] upon Sb_2S_3 surface justifies the improvement of the wettability behavior as observed from the water contact angle measurements (cf. Figure 2). This polar group casted also a profound influence on the photoelectroactivity enhancement as it favored the interaction of the H_3O^+ ions onto the treated film's surface. Such interaction is very likely to be electrostatic and the van der Waals interaction, which exists at any interface solid/liquid,[39] is probably the one prevailing in the absence of this polar group. Since electrostatic interaction is stronger than van der Waals', the attraction of the H_3O^+ ions to the film's surface is enhanced. As a result, the photogenerated electrons transfer at the interface Sb_2S_3/electrolyte is facilitated, and thus increasing the photocurrent density values as behold in Figure 1.

As a final remark, to the best of our knowledge, this is the very first time that the plasma treatment approach has been reported for the photoelectroactivity improvement of bare Sb_2S_3 films applied as photocathode for H_2 production in PEC. Moreover, the plasma treatment methodology developed here is of importance as it can be useful for the photoelectroactivity enhancement of other chalcogenide materials which may present a hydrophobic surface.

3. Conclusions

This work brings the novel development of a fast nitrogen plasma treatment for the further photoelectroactivity improvement of bare Sb_2S_3 photocathodes towards H_2 production. In comparison to the non-plasma film, the photoelectrochemical assessment of the Sb_2S_3 films revealed a 24-fold increase of cathode photocurrent density values for the film treated under nitrogen plasma for 10 s. Such remarkable improvement is connected with the film's surface turning from superhydrophobic (non-plasma treatment) to hydrophilic (plasma treatment), as observed by the water angle measurements. According to XPS analysis, the hydrophilic behavior of the Sb_2S_3 films might be due to the presence of the S–N polar group originated by the nitrogen plasma treatment. We believe that in the future this new approach can potentially pave the way for even

greater progress in the photoelectroactivity of Sb_2S_3 films for PEC and/or photovoltaic cell applications.

Acknowledgements

We would like to thank the financial support provided by the São Paulo Research Foundation (FAPESP) whose grant numbers are: 2016/12681-0 (M.A.A.), 2013/07296-2 (CEPID/CDMF), 2017/11986-5 (FAPESP/SHELL) and 2018/16401-8 (L.H.M.). We are also grateful to Professor Valmor R. Mastelaro for the XPS measurements, and Professor Sandra A. Cruz and Luíza M. Bozzo for the contact angle measurements.

Conflict of Interest

The authors declare no conflict of interest.

Keywords: antimony(III) sulfide · hydrogen · surface modification · nitrogen plasma · energy conversion

[1] X. Li, J. Yu, J. Low, Y. Fang, J. Xiao, X. Chen, *J. Mater. Chem. A* **2015**, *3*, 2485–2534.
[2] X. Huang, H. Woo, P. Wu, Q. Wang, G. Tan, *J. Alloys Compd.* **2019**, *777*, 866–871.
[3] L. Jiang, J. Chen, Y. Wang, Y. Pan, B. Xiao, N. Ouyang, F. Liu, *J. Electrochem. Soc.* **2018**, *165*, H1052-H1058.
[4] M. I. Medina-Montes, Z. Montiel-González, F. Paraguay-Delgado, N. R. Mathews, X. Mathew, *J. Mater. Sci. Mater. Electron.* **2016**, *27*, 9710–9719.
[5] H. Lei, J. Chen, Z. Tan, G. Fang, *Sol. RRL.* **2019**, *3*, 1900026.
[6] A. D. DeAngelis, K. C. Kemp, N. Gaillard, K. S. Kim, *ACS Appl. Mater. Interfaces* **2016**, *8*, 8445–8451.
[7] X. Lu, Z. Liu, *Dalton Trans.* **2017**, *46*, 7351–7360.
[8] Q. Cai, Z. Liu, C. Han, Z. Tong, C. Ma, *J. Alloys Compd.* **2019**, *795*, 319–326.
[9] L. Meng, X. Zhou, S. Wang, Y. Zhou, W. Tian, P. Kidkhunthod, S. Tunmee, Y. Tang, R. Long, Y. Xin, L. Li, *Angew. Chem. Int. Ed.* **2019**, *58*, 2–10.
[10] A. Bismarck, M. E. Kumru, J. Springer, *J. Colloid Interface Sci.* **1999**, *210*, 60–72.
[11] M. L. Steen, L. Hymas, E. D. Havey, N. E. Capps, D. G. Castner, E. R. Fisher, *J. Membr. Sci.* **2001**, *188*, 97–114.
[12] Q. Wei, Y. Liu, D. Hou, F. Huang, *J. Mater. Process. Technol.* **2007**, *194*, 89–92.
[13] M. Calixto-Rodriguez, F. Castillo, H. Martínez, Y. Peña, A. Sanchez-Juarez, *J. Phys. Conf. Ser.* **2010**, *207*, 12019.
[14] M. Calixto-Rodriguez, H. Martínez, Y. Peña, O. Flores, H. E. Esparza-Ponce, A. Sanchez-Juarez, J. Campos-Alvarez, P. Reyes, *Appl. Surf. Sci.* **2010**, *256*, 2428–2433.
[15] S. Inbakumar, P. M. Andavan, *Rasayan J. Chem.* **2017**, *10*, 507–512.
[16] M. A. de Araújo, F. W. S. Lucas, L. H. Mascaro, *J. Solid State Electrochem.* **2020**, *24*, 389–399.
[17] L. M. Peter, *Chem. Rev.* **1990**, *90*, 753–769.
[18] P. Bayliss, W. Nowacki, *Zeitschrift für Krist.* **1972**,135, 308–315.
[19] S. Samipour, H. Taghvaei, D. Mohebbi-Kalhori, M. R. Rahimpour, *Surf. Innov.* **2020**, *8*, 76–88.
[20] R. R. Deshmukh, N. V. Bhat, *Mat. Res. Innov.* **2003**, *7*, 283–290.
[21] F. Dauzvardis, A. Knapp, K. N. D. Shein, G. Lisensky, *J. Chem. Educ.* **2020**, *97*, 184–189.
[22] J. D. Musgraves, J. Hu, L. Calvez, Springer Handbook of Glass, Springer, Switzerland, **2019**, pp. 1599.
[23] E. Dutková, M. J. Sayagués, C. Real, A. Zorkovská, P. Baláž, A. Šatka, J. Kováč, J. Ficeriová, *Acta Phys. Pol. A* **2014**, *126*, 943–946.
[24] M. Deng, S. Li, W. Hong, Y. Jiang, W. Xu, H. Shuai, H. Li, W. Wang, H. Hou, X. Ji, *RSC Adv.* **2019**, *9*, 15210–15216.
[25] Z. Zhang, J. Zhao, M. Xu, H. Wang, Y. Gong, J. Xu, *Nanotechnology* **2018**, *29*, 335401.
[26] Q. Wang, Y. Lai, F. Liu, L. Jiang, M. Jia, *Energy Technol.* **2019**, *7*, 1900928.
[27] C. Gao, M. Xu, B. K. Ng, L. Kang, L. Jiang, Y. Lai, F. Liu, *Mater. Lett.* **2017**, *195*, 186–189.
[28] G.-H. He, C.-J. Liang, Y.-D. Ou, D.-N. Liu, Y.-P. Fang, Y.-H. Xu, *Mater. Res. Bull.* **2013**, *48*, 2244–2249.
[29] L. Guo, B. Zhang, S. Li, Q. Zhang, M. Buettner, L. Li, X. Qian, F. Yan, *APL Mater.* **2019**, *7*, 41105.
[30] P. K. Chow, E. Singh, B. C. Viana, J. Gao, J. Luo, J. Li, Z. Lin, A. L. Elías, Y. Shi, Z. Wang, M. Terrones, N. Koratkar, *ACS Nano* **2015**, *9*(3), 3023–3031.
[31] J. Sharma, D. S. Downs, Z. Iqbal, F. J. Owens, *J. Chem. Phys.* **1977**, *67*, 3045.
[32] Q. Sun, W.-J. Li, Z.-W. Fu, *Solid State Sci.* **2010**, *12*, 397–403.
[33] C. Guorong, H. Zheng, X. Jun, C. Jijian, *J. Non-Cryst. Solids* **2001**, *288*, 226–229.
[34] A. D. Nguyen, T. K. Nguyen, C. T. Le, S. Kim, F. Ullah, Y. Lee, S. Lee, K. Kim, D. Lee, S. Park, J.-S. Bae, J. I. Jang, Y. S. Kim, *ACS Omega* **2019**, *4*, 21509–21515.
[35] J. Jiang, Q. Zhang, A. Wang, Y. Zhang, F. Meng, C. Zhang, X. Feng, Y. Feng, L. Gu, H. Liu, L. Han, *Small* **2019**, *15*, 1901791.
[36] C.-M. Chan, T.-M. Ko, H. Hiraoka, *Surf. Sci. Rep.* **1996**, *24*, 1–54.
[37] D. J. Masruroh, D. H Santjojo, M. Heraniawati, A. Abdillah, T. N. Zafirah, E. Maulana, S. P. Sakti, *Int. J. GEOMATE* **2019**, *17*, 68–73.
[38] R. H. Findlay, M. H. Palmer, A. J. Downs, R. G. Egdell, R. Evans, *Inorg. Chem.* **1980**, *19*, 1307–1314.
[39] P. Snapp, J. M. Kim, C. Cho, J. Leem, M. F. Haque, S. Nam, *NPG Asia Mater.* **2020**, *12*, 1–22.

Manuscript received: March 3, 2020
Revised manuscript received: April 30, 2020

ARTICLES

Works a treat: The non-plasma Sb_2S_3 film presents poor wettability and reduced photoelectroactivity for H_2 evolution. Once treated under nitrogen plasma, the film's surface becomes hydrophilic and the photoelectrochemical response is greatly improved. Chemical analysis shows the formation of S–N polar groups on the surface of the treated Sb_2S_3 film. The S–N group probably plays the major role in the enhancement of the wettability and photoelectroactivity.

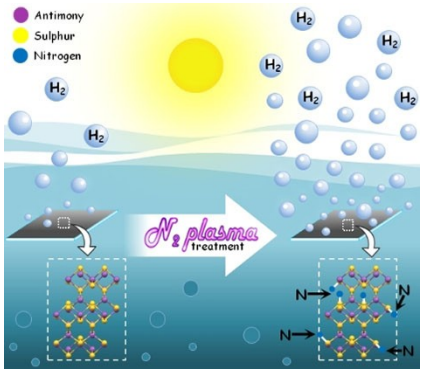

*M. A. De Araújo, Prof. Dr. L. H. Mascaro**

SPACE RESERVED FOR IMAGE AND LINK

Share your work on social media! *ChemElectroChem* has added Twitter as a means to promote your article. Twitter is an online microblogging service that enables its users to send and read short messages and media, known as tweets. Please check the pre-written tweet in the galley proofs for accuracy. If you, your team, or institution have a Twitter account, please include its handle @username. Please use hashtags only for the most important keywords, such as #catalysis, #nanoparticles, or #proteindesign. The ToC picture and a link to your article will be added automatically, so the **tweet text must not exceed 250 characters**. This tweet will be posted on the journal's Twitter account (follow us @ChemElectroChem) upon publication of your article in its final (possibly unpaginated) form. We recommend you to re-tweet it to alert more researchers about your publication, or to point it out to your institution's social media team.

ORCID (Open Researcher and Contributor ID)

Please check that the ORCID identifiers listed below are correct. We encourage all authors to provide an ORCID identifier for each coauthor. ORCID is a registry that provides researchers with a unique digital identifier. Some funding agencies recommend or even require the inclusion of ORCID IDs in all published articles, and authors should consult their funding agency guidelines for details. Registration is easy and free; for further information, see http://orcid.org/.

Moisés A. De Araújo
Prof. Dr. Lucia H. Mascaro http://orcid.org/0000-0001-6908-1097